

HECHT, AXEL; CARSTENSEN, CARSTEN; ZARRABI, DARIUS

Adaptive Discretisation of Shell Problems

A seven parameter Reissner-Mindlin shell kinematic is employed for a elastoplastic material with hardening. The resulting nonlinear minimization problem is discretised within a finite element method on the mid surface of the shell. A posteriori error estimates are discussed and related adaptive algorithms are presented. Numerical examples illustrate the theoretical results.

1. Model Problem

The model problem investigated is a cylindrical shell with the thickness t . It occupies the domain $\mathcal{S}(z, \varphi, r) = \{(1+r)\cos\varphi, -(1+r)\sin\varphi, z\}$, $-t/2 < r < t/2$, $0 < z < L$, $0 < \varphi \leq 2\pi$ and r being the distance from shell mid surface $\mathcal{S}(r=0)$. The displacement U^{3D} on \mathcal{S} is given in terms of functions on the mid surface. The resulting displacement is used in elastoplasticity for small displacements. The displacement U^{3D} is described by a set of 7 functions, or a 7 parameter kinematics,

$$U^{3D} = (u - r\theta) \mathbf{e}_z + (v - r\phi) \mathbf{e}_\varphi + (w - r\psi - r^2\eta) \mathbf{e}_r. \quad (1)$$

2. Principle of Virtual Work

For an arbitrary material law, the principle of virtual work reads

$$\int_{\mathcal{S}} \boldsymbol{\sigma} : \boldsymbol{\epsilon}(V^{3D}) d\mathcal{S} - \int_{\mathcal{S}} \mathbf{f} \cdot V^{3D} d\mathcal{S} = 0 \quad (V^{3D} \in H^1(\mathcal{S})^3). \quad (2)$$

As the testfunctions obey the kinematics, this yields to a strong formulation consisting of seven partial differential equations,

$$\begin{aligned} \int_{-t/2}^{t/2} \frac{1}{\chi} (f_z + \sigma_{zz,z} + \chi \sigma_{z\varphi,\varphi}) dr &= 0, & \int_{-t/2}^{t/2} \frac{1}{\chi} (rf_z - r\sigma_{zz,z} - r\chi \sigma_{z\varphi,\varphi} + \sigma_{zr}) dr &= 0, \\ \int_{-t/2}^{t/2} \frac{1}{\chi} (f_\varphi + \sigma_{\varphi z,z} + \chi \sigma_{\varphi\varphi,\varphi} + \chi \sigma_{\varphi r}) dr &= 0, & \int_{-t/2}^{t/2} \frac{1}{\chi} (rf_\varphi - r\sigma_{\varphi z,z} - r\chi \sigma_{\varphi\varphi,\varphi} + (1-r\chi)\sigma_{\varphi r}) dr &= 0, \\ \int_{-t/2}^{t/2} \frac{1}{\chi} (f_r + \sigma_{rz,z} + \chi \sigma_{r\varphi,\varphi} - \chi \sigma_{\varphi\varphi}) dr &= 0, & \int_{-t/2}^{t/2} \frac{1}{\chi} (rf_r - r\sigma_{rz,z} - r\chi \sigma_{r\varphi,\varphi} + r\chi \sigma_{\varphi\varphi} + \sigma_{rr}) dr &= 0, \\ \int_{-t/2}^{t/2} \frac{1}{\chi} (r^2 f_r - 2r\sigma_{rr} + r^2(\sigma_{rz,z} - \chi \sigma_{\varphi\varphi} + \chi \sigma_{r\varphi,\varphi})) dr &= 0. \end{aligned}$$

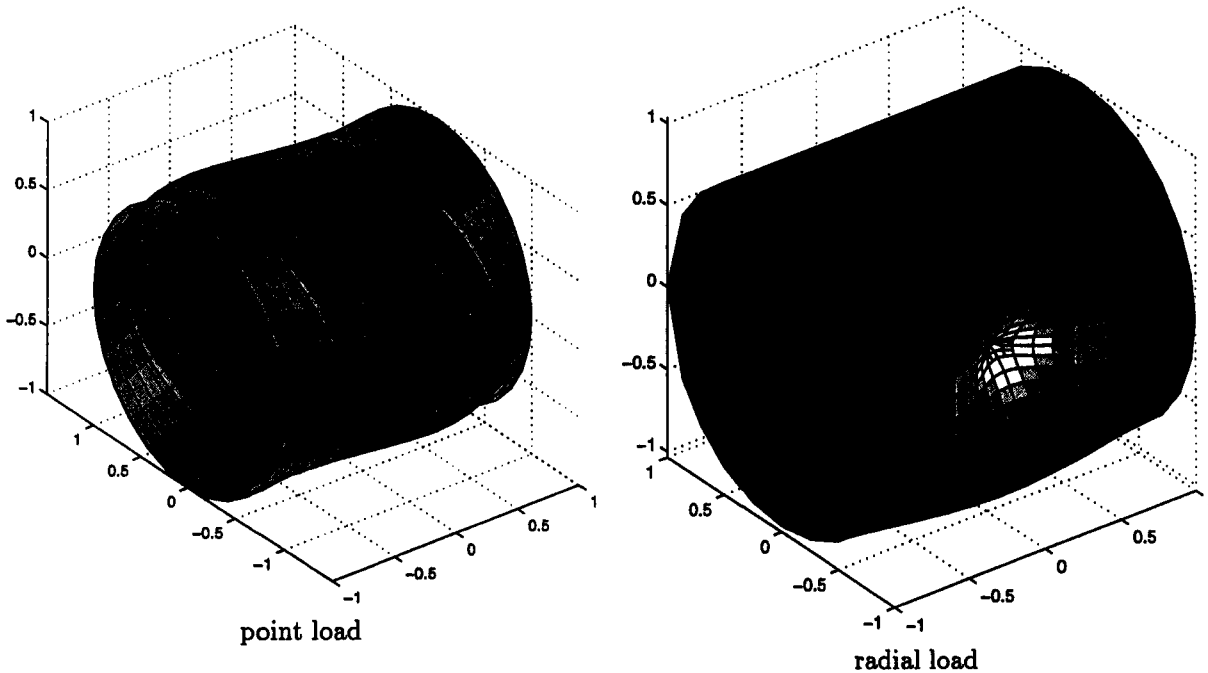
3. A Posteriori Error Indicator

A residual-based a posteriori error estimate can be obtained from the strong formulation above with element contributions η_T and edge contributions η_E . The constants in this reliable a posteriori error estimate depend on the thickness, and efficiency is still open. The local contributions are chosen as error indicator for the adaptive refinement algorithm. Both η_T and η_E are given for arbitrary discrete stresses Σ

$$\begin{aligned} \eta_T^2 &= h_T^2 \int_T \left\{ \left| \int_{-i/2}^{i/2} (f_1 - \Sigma_{zz,s} - \chi \Sigma_{\varphi s, \varphi})(1+r) dr \right|^2 \right. \\ &+ \dots \\ &+ \left| \int_{-i/2}^{i/2} (r(\Sigma_{ss,s} + \chi \Sigma_{\varphi s, \varphi}) - \Sigma_{rs})(1+r) dr \right|^2 \\ &+ \dots \\ &+ \left. \left| \int_{-i/2}^{i/2} (r^2(\Sigma_{rs,s} + \chi \Sigma_{r\varphi, \varphi} - \chi \Sigma_{\varphi\varphi}) - 2r \Sigma_{rr})(1+r) dr \right|^2 \right. \\ &\eta_B^2 = h_B^2 \int_B \left\{ \left| \int_{-i/2}^{i/2} \left[\Sigma \cdot \begin{pmatrix} n_s \\ \chi n_\varphi \\ 0 \end{pmatrix} \right] (1+r) dr \right|^2 \right. \\ &+ \left| \int_{-i/2}^{i/2} \left[\Sigma \cdot \begin{pmatrix} n_s \\ \chi n_\varphi \\ 0 \end{pmatrix} \right] r (1+r) dr \right|^2 \\ &+ \left. \left| \int_{-i/2}^{i/2} [\Sigma_{rs} \cdot n_s + \chi \Sigma_{r\varphi} \cdot n_\varphi] r^2 (1+r) dr \right|^2 \right. \\ &\chi = 1/(1+r) \end{aligned}$$

4. Numerical Experiments

We discretised the model problem with Q1 finite elements on rectangular grids aligned both to the φ - and z -axis. Due to the adaptive refinement algorithm the discretisation allows hanging nodes. We have done numerical experiments with a point load, a radial load as well as a load tangential to the midsurface. Shown here are one example with point load as well as one example with radial load.



The brightness indicates van Mises stresses $\|\text{dev}\Sigma\|$. The radial load is given by $f = (z^2 - 1)^4 \cos(2\varphi) e_r$. It can be seen that for both loads the adaptive refinement algorithm results in finer meshes at areas with high changes in stresses.

Further work will be done in applying the a posteriori error indicator to more general material laws in elastoplasticity and a broader range of finite element discretisations.

Addresses: AXEL HECHT, PROF. DR. CARSTEN CARSTENSEN, DARIUS ZARRABI Ludewig-Meyn-Str. 4
 Christian Albrechts Universität zu Kiel
 24089 Kiel Germany